INDIAN JOURNAL OF SCIENCE AND TECHNOLOGY

RESEARCH ARTICLE

Magnetohydrodynamic Micropolar Fluid Squeeze Film Lubrication between Stepped Porous Parallel Plates

N B Naduvinamani[1]*, Ashwini Angadi[2]

1 Professor, Department of Mathematics, Gulbarga University, Kalaburagi, 585106, Karnataka, India
2 Research Scholar, Department of Mathematics, Gulbarga University, Kalaburagi-, Karnataka, 585106, India

OPEN ACCESS

Received: 07-06-2022

Accepted: 17-08-2022

Published: 29-10-2022

Citation: Naduvinamani NB, Angadi A (2022) Magnetohydrodynamic Micropolar Fluid Squeeze Film Lubrication between Stepped Porous Parallel Plates. Indian Journal of Science and Technology 15(40): 2066-2076. https://doi.org/10.17485/IJST/v15i40.1203

* **Corresponding author**.

naduvinamaninb@yahoo.co.in

Funding: None

Competing Interests: None

Published By Indian Society for Education and Environment (iSee)

ISSN
Print: 0974-6846
Electronic: 0974-5645

Abstract

Objectives: The primary goal of this paper is to study the influence of MHD and micropolar fluid on the squeeze film lubrication between stepped porous parallel plates. **Method:** The non-Newtonian micropolar fluid MHD Reynolds type equation is derived by considering the flow of micropolar fluid in the porous matrix as described by Darcy's law, as well as microstructure additives and magnetic effects associated with the magnetization of the fluid. The numerical solutions are presented graphically for the MHD squeeze film characteristics for various values of coupling number parameter, characteristic material length, and magnetic Hartmann number. **Findings:** According to the results, the micropolar fluid and the magnetic effects significantly influence the squeeze film characteristics. Comparing the MHD micropolar fluid impact on the squeeze film lubrication with the corresponding Newtonian and non-magnetic cases, we observe that there is a significant increase in the approaching time and the load-carrying capability. The increase in the step height decreases the squeezing film time. **Novelty:** The original research was conducted on the magneto-hydrodynamic micropolar fluid squeeze film lubrication between stepped porous parallel plates which has not been studied so far. The effect of applied magnetic field is to enhance the load carrying capacity and delayed time of approach which are the most desirable characteristics for improving the bearing performance.

Keywords: Squeeze Film; Stepped plates; Magnetohydrodynamic; Porous; Micropolar

1 Introduction

Gears, machine tools, gyroscopes, wet-clutch plates, automotive engines, aircraft engines, and the mechanics of synovial joints in humans and animals are only a few of the applications for squeeze film bearings in applied sciences and industrial engineering. The lubricating surfaces move towards each other in the normal direction, forming a squeeze film, developing positive pressure, and thus supporting a load. As the two surfaces move towards each other, a viscous lubricant between them cannot easily be

squeezed out. This process has a cushioning effect on the bearing. The time it takes for the lubricant to squeeze out depends on the configuration of the bearing surface, properties of fluids, the load applied, and other factors. At the earlier stage, numerous researchers have analyzed the Newtonian fluid squeeze film lubrication of bearings. Researchers were attracted to porous bearings by their simple structure and low cost. The use of porous bearings in mounting horsepower motors is widespread, including in water pumps, tape recorders, vacuum cleaners, sewing machines, shaving machines, record players, coffee grinders, hair dryers, generators, and distributors. The squeezing flow has been analyzed by various researchers between parallel and rectangular plates. Hays [(1)] analysed the normal approach of curved and flat rectangular plates separated by a thin film of lubricant. Hai Wu [(2)] theoretically studied the squeeze film between porous rectangular plates. The flow between parallel plates receding or approaching each other symmetrically is investigated by Singh et.al. [(3)].Characteristics of squeeze film between porous parallel stepped plates for micropolar fluid have been theoretically described by Siddanagouda [(4)]. Naduvinamani et.al. [(5)] presented the effect of pressure-dependent viscosity on the squeeze film behavior between rough parallel plates with couplestress fluid. Patel and Deheri [(6)] studied the impact of surface roughness and slip velocity on the performance of the Jenkins model based ferrofluid squeeze film in curved annular plates. Hanamagowda et.al. [(7)] proposed the study of the impact of pressure-dependent viscosity and micropolar fluids on squeeze film circular stepped plates. Madalli [(8)] analyzed the viscosity-dependent parameters of non-Newtonian couplestress fluid between parallel porous plates. Hanumagowda et.al. [(9)] presented the squeeze film lubrication between circular stepped plates with the combined effect of pressure-dependent viscosity and surface roughness. Anagod et.al. [(10)] investigated the squeeze film behavior of rough elliptical plates with micropolar fluid. Jahan et.al. [(11)] and Hanumagowda et.al. [(9)] derived the stochastic Reynolds equation to analyze the piezo viscous dependency effect on the squeeze film behavior of the rough annular plates and porous circular stepped plates. Goud et.al. [(12)] studied the mass and heat transport phenomena associated with micropolar fluid flow over a vertical Riga plate.

The microploar fluid model was first introduced by Eringen [(13)]. The study of fluids containing tiny particles, such as polymers, suspended fluids, paints, animal blood, lubricants with additives, etc., can be done using Eringen's [(13)] micropolar fluids theory. Numerous industrial applications of the research of micropolar fluids include the extrusion of polymer fluids, colloidal and suspension solutions, the cooling of metallic plates, exotic lubricants, and the solidification of liquid crystals. The MHD lubrication has been developed because a liquid metal lubricated bearing's load can be enhanced when a magnetic field is introduced. Because of their high conductivity, liquid metals have recently attracted considerable attention. Several types of magnetohydrodynamic bearings have been developed in recent years. The study of the interaction between conducting fluids and electromagnetic phenomena is known as magnetohydrodynamics. The magnetic field is a major element in conditioning and controlling tribological properties. According to recent research, applying a magnetic field to the friction contact can increase the partial pressure of oxygen on the rubbing surface, resulting in the formation of a friction-reducing oxidation film. Application of magnetohydrodynamic lubrication to liquid metals has been analysed by Hughes [(14)]. Kuzma et.al. [(15)] investigated experimentally and theoretically themagnetohydrodynamic squeeze films and Hamza [(16)] studied the motion of an electrically conducting fluid film squeezed between two parallel disks. Lin et.al. [(17)] performed squeeze film characteristics between curved circular plates lubricated with an electrically conducting non-Newtonian fluid in the presence of external magnetic fields. Saeed Islam et.al. [(18)] investigated the heat transmission and the magnetohydrodynamic flow of a micropolar hybrid nanofluid between two surfaces inside a rotating system. Halambi and Hanumagowda [(19)] theoretically investigated the effect of micropolar lubricant on the squeeze film lubrication between elliptical plates under the influence of an applied magnetic field. Shah et.al. [(20)] analysed the flow of non-isothermal micropolar fluid over a nonlinear extending surface with Cattaneo-Christov heat flux model. Later shah et.al. [(21)] investigated the entropy generation in MHD flows of water based silver and copper nanofluids. Biradar et.al. [(22)] carried out the study on the squeeze film characteristics by considering the MHD and couplestress effect on the porous curved annular circular plates. The numerical analysis of MHD boundary layer non-Newtonian micropolar fluid due to an exponentially curved stretching sheet is derived by Hong Shi et.al. [(23)]. Agarwal et.al. [(24)] studied the magnetohydrodynamic micropolar fluid flow in a permeable channel with thermal radiation. Ullah et.al. [(25)] analyzed the flow of micro-polar nano-fluid between parallel plates with the effects of electric and magnetic fields.

As per the literature known, so far, no research has been conducted on the MHD micropolar fluid squeeze film lubrication between porous parallel stepped plates. As a result, this study attempted to analyze the influence of MHD on the squeeze film lubrication between porous parallel stepped plates lubricated with micropolar fluid using Eringen's [(14)] micropolar fluid theory.

2 Mathematical analysis

Figure 1 shows the physical geometry of the squeeze film lubrication of conducting micropolar fluid between parallel porous stepped plates, where the upper stepped plate is moving closer to the lower porous parallel plate with a velocity V . An external magnetic field of strength B_o is applied along the y-direction. The basic equations describing the flow of an incompressible non-Newtonian micropolar fluid with an external magnetic field B_o under the assumption of hydrodynamic lubrication for the

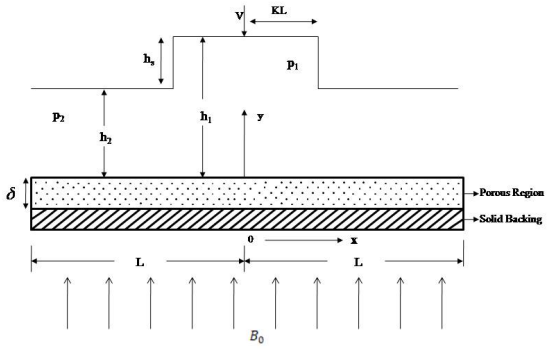

Fig 1. Geometry of the considered problem

thin film are given by

$$\frac{\partial v}{\partial y}+\frac{\partial u}{\partial x}=0 \tag{1}$$

$$\left(\frac{\chi}{2}+\mu\right)\frac{\partial^2 u}{\partial y^2}+\chi\frac{\partial v_1}{\partial y}-\sigma B_0^2 u=\frac{\partial p}{\partial x} \tag{2}$$

$$\frac{\partial p}{\partial y}=0 \tag{3}$$

$$\gamma\frac{\partial^2 v_1}{\partial y^2}-\chi\frac{\partial u}{\partial y}-2\chi v_1=0 \tag{4}$$

Where *(u, v)* are the lubricant velocity components along x and y directions respectively, v_1 is micro-rotational velocity, χ and $\gamma$are micropolar fluid viscosity coefficients and $\mu$is the classical viscosity coefficient.

The pertinent boundary conditions are

i. At $y = h$ (upper surface of the bearing)

$$u=0, v=\frac{\partial h}{\partial t}$$
$$v_1=0 \tag{5a}$$

ii. At $y = 0$ (lower surface of the bearing)

$$u=0, v=v^*$$

$$v_1=0 \tag{5b}$$

From Eqs. (2) and (4) eliminate v_1, we obtain

$$\frac{\partial^4 u}{\partial y^4}-\alpha\frac{\partial^2 u}{\partial y^2}+\beta u=f(x) \tag{6}$$

where, $\alpha = \frac{2(2\mu\chi+\gamma\sigma B_0^2)}{\gamma(2\mu+\chi)}, \beta = \frac{4\chi\sigma B_0^2}{\gamma(2\mu+\chi)}$ and $f(x) = \frac{-4\chi}{\gamma(2\mu+\chi)}\frac{\partial p}{\partial x}$

Solution of Eq. (6) is

$$u = C_1\,\mathrm{Cosh}\,(A_1 y) + C_2\,\mathrm{Sinh}\,(A_1 y) + C_3\,\mathrm{Cosh}\,(A_2 y) + C_4\,\mathrm{Sinh}\,(A_2 y) + \frac{f}{\beta} \tag{7}$$

By using the expression for u and integrating equation (2), we obtain

$$v_1 = g_1 C_1\,\mathrm{Sinh}\,(A_1 y) + g_1 C_2\,[\mathrm{Cosh}\,(A_1 y) - 1] + g_2 C_3\,\mathrm{Sinh}\,(A_2 y) + g_2 C_4\,[\mathrm{Cosh}\,(A_2 y) - 1] \tag{8}$$

Expression for micro rotational velocity is given in Eq. (8) and is solved by integrating Eq. (4) with the expression of u

$$\begin{aligned} v_1 =& C_1\frac{A_1}{2\chi}\,\mathrm{Sinh}\,(A_1 y)\,[\gamma g_1 A_1 - \chi] + C_2\frac{A_1}{2\chi}\,\mathrm{Cosh}\,(A_1 y)\,[\gamma g_1 A_1 - \chi] + \\ & C_3\frac{A_2}{2\chi}\,\mathrm{Sinh}\,(A_2 y)\,[\gamma g_2 A_2 - \chi] + C_4\frac{A_2}{2\chi}\,\mathrm{Sinh}\,(A_2 y)\,[\gamma g_2 A_2 - \chi] \end{aligned} \tag{9}$$

where, $A_1 = \left[\frac{\alpha+\sqrt{\alpha^2-4\beta}}{2}\right]^{1/2}, A_2 = \left[\frac{\alpha-\sqrt{\alpha^2-4\beta}}{2}\right]^{1/2}, g_1 = \frac{2\sigma B_0^2-(2\mu+\chi)A_1^2}{2A_1}, g_2 = \frac{2\sigma B_0^2-(2\mu+\chi)A_2^2}{2A_2}$

Expression of u is obtained which by determining the integrating constants C_1, C_2, C_3 and C_4 using Eqs (7)-(9) and boundary conditions (5a)-(5b). Use of expression for u and integrating continuity equation (1) and applying the relative boundary conditions across film thickness give rise to the non-Newtonian MHD micropolar fluid Reynolds equation in the form

$$\frac{\partial}{\partial x}\left[\frac{a-b}{\sigma B_0^2 A_1 A_2 (c-d)}\cdot\frac{\partial p}{\partial x}\right] = -V - v^* \tag{10}$$

Where $a = g_1 A_1\,\mathrm{Sinh}\left(\frac{A_1 h}{2}\right)\left(A_2 h\,\mathrm{Cosh}\left(\frac{A_2 h}{2}\right) - 2\,\mathrm{Sinh}\left(\frac{A_2 h}{2}\right)\right)$

$b = g_2 A_2\,\mathrm{Sinh}\left(\frac{A_2 h}{2}\right)\left(A_1 h\,\mathrm{Cosh}\left(\frac{A_1 h}{2}\right) - 2\,\mathrm{Sinh}\left(\frac{A_1 h}{2}\right)\right)$

$c = g_1\,\mathrm{Cosh}\left(\frac{A_2 h}{2}\right)\mathrm{Sinh}\left(\frac{A_1 h}{2}\right), d = g_2\,\mathrm{Cosh}\left(\frac{A_1 h}{2}\right)\mathrm{Sinh}\left(\frac{A_2 h}{2}\right)$

The modified Darcy velocity vector

$$\vec{q} = (u^*, v^*) = \frac{-\phi^*}{\mu+\chi}\nabla p^* \tag{11}$$

where p^* is pressure and $\phi*$is permeability of the porous matrix. As a result of the continuity of the fluid, the p^* satisfies the Laplace equation

$$\frac{\partial^2 p^*}{\partial x^2} + \frac{\partial^2 p^*}{\partial y^2} = 0 \tag{12}$$

Over the porous layer thickness δ, integrating eqn.(12) with respect to y then applying solid backing boundary condition $\left(\frac{\partial p^*}{\partial y} = 0\right)$ at y = -δ, we obtain

$$\left(\frac{\partial p^*}{\partial y}\right)_{y=0} = \int_{-\delta}^{0}\frac{\partial^2 p^*}{\partial x^2}dy \tag{13}$$

At (y = 0) the porous interface, Eq. (13) becomes

$$\left(\frac{\partial p^*}{\partial y}\right)_{y=0} = -\delta\frac{\partial^2 p}{\partial x^2} \tag{14}$$

The velocity component v^* at the interface (y = 0) is given by

$$v^*|_{y=0} = \frac{\phi^*\delta}{\mu+\chi}\left(\frac{\partial^2 p}{\partial x^2}\right) \tag{15}$$

Substituting this in Eq. (11), for micropolar fluids, the modified Reynolds equation is obtained as follows

$\frac{\partial}{\partial x}\left[\left(\frac{a-b}{\sigma B_0^2 A_1 A_2 (c-d)}+\frac{\phi^* \delta}{\mu+\chi}\right)\cdot\frac{\partial p}{\partial x}\right]=-V$

The non-dimensional quantities are,

$\bar{x}=\frac{x}{L},\bar{h}=\frac{h}{h_2},\overline{\alpha}=h_2^2\alpha,\overline{\beta}=h_2^4\beta,\overline{R_1}=h_2R_1,\overline{R_2}=h_2R_2,\overline{g_1}=h_2\,g_1,\overline{g_2}=h_2g_2,\psi=\frac{K\delta}{h_2^3},\bar{t}=\frac{Ut}{L},\overline{p}=\frac{ph_0^3}{\mu L^2 V}$

The modified Reynolds equation attained in non-dimensional form is

$$\frac{\partial}{\partial\bar{x}}\left[\left(F\left(\bar{h},N,L,M_0\right)+\psi\left(\frac{1-N^2}{1+N^2}\right)\right)\frac{\partial\overline{p}}{\partial\bar{x}}\right]=-1 \tag{16}$$

where $F\left(\bar{h},N,L,M_0\right)=\frac{\bar{a}-\bar{b}}{M_0^2\overline{A_1}\overline{A_2}(\bar{c}-\bar{d})}$

$\bar{a}=\bar{g}_1\bar{A}_1\,\mathrm{Sinh}\left(\frac{\overline{A_1}\bar{h}}{2}\right)\left(\overline{A_2}\bar{h}\,\mathrm{Cosh}\left(\frac{\overline{A_2}\bar{h}}{2}\right)-2\,\mathrm{Sinh}\left(\frac{\overline{A_2}\bar{h}}{2}\right)\right)$

$\bar{b}=\overline{g_2}\overline{A_2}\,\mathrm{Sinh}\left(\frac{\overline{A_2}\bar{h}}{2}\right)\left(\overline{A_1}\bar{h}\,\mathrm{Cosh}\left(\frac{\overline{A_1}\bar{h}}{2}\right)-2\,\mathrm{Sinh}\left(\frac{\overline{A_1}\bar{h}}{2}\right)\right)$

$\bar{c}=\overline{g_1}\,\mathrm{Cosh}\left(\frac{\overline{A_2}\bar{h}}{2}\right)\mathrm{Sinh}\left(\frac{\overline{A_1}\bar{h}}{2}\right),\bar{d}=\overline{g_2}\,\mathrm{Cosh}\left(\frac{\overline{A_1}\bar{h}}{2}\right)\mathrm{Sinh}\left(\frac{\overline{A_2}\bar{h}}{2}\right)$

$\overline{g_1}=g_1h_2=\frac{M_0^2(1-N^2)-\overline{A_1}^2}{2N^2\overline{A_1}},\ \overline{g_2}=g_2h_2=\frac{M_0^2(1-N^2)-\overline{A_2}^2}{2N^2\overline{A_2}}$

$\overline{A_1}=h_2A_1=\left(\frac{\bar{\alpha}+\sqrt{\bar{\alpha}^2-4\bar{\beta}}}{2}\right)^{1/2},\overline{A_2}=h_2A_2=\left(\frac{\bar{\alpha}-\sqrt{\bar{\alpha}^2-4\bar{\beta}}}{2}\right)^{1/2}$

$\bar{\alpha}=\alpha h_2^2=\frac{N^2+M_0^2(1-N^2)L^2}{L^2},\bar{\beta}=\beta h_2^4=\frac{N^2M_0^2}{L^2},N=\left(\frac{\chi}{2\mu+\chi}\right)^{1/2},L=\left(\frac{(\gamma/4\mu)^{1/2}}{h_2}\right),M_0=B_0h_2\left(\frac{\sigma}{\mu}\right)^{1/2}$

where N is dimensionless coupling number, L is the characteristic material length. Dimension of L is of length and can be recognized as a size of microstructure additives available in the lubricant $h_0$is initial film thickness and M_0 is magnetic Hartmann parameter.

The pertinent pressure boundary conditions are

$$\overline{p_1}=\overline{p_2}\ \text{at}\ \bar{x}=K \tag{17a}$$

$$\overline{p_2}=0\ \text{at}\ \bar{x}=1 \tag{17b}$$

The film pressure in non-dimensional form is obtained by solving Eq.(16) with the conditions given in Eqs.(17a) and (17b).

$$\overline{p_1}=\frac{K^2-\bar{x}^2}{2\left[F_1\left(\bar{h}_1,N,L,M_0\right)+\psi\left(\frac{1-N^2}{1+N^2}\right)\right]}+\frac{1-K^2}{2\left[F_2\left(1,N,L,M_0\right)+\psi\left(\frac{1-N^2}{1+N^2}\right)\right]} \tag{18}$$

$$\overline{p_2}=\frac{1-\bar{x}^2}{2\left[F_2\left(1,N,L,M_0\right)+\psi\left(\frac{1-N^2}{1+N^2}\right)\right]} \tag{19}$$

The load-carrying capacity w is given by

$$w=2b\int_0^{KI}p_1dx+2b\int_{KL}^{L}p_2dx \tag{20}$$

The load capacity W in non-dimensional form is:

$$W=\frac{3wh_0^3}{2\mu bVL^3}=\left[\frac{K^3}{F_1\left(\overline{h_1},N,L,M_0\right)+\psi\left(\frac{1-N^2}{1+N^2}\right)}+\frac{1-K^3}{F_2\left(1,N,L,M_0\right)+\psi\left(\frac{1-N^2}{1+N^2}\right)}\right] \tag{21}$$

Letting $V=-\frac{dh_2}{dt}$ in Eq. (21), the squeezing time required to reduce the initial thickness $h_0$of $h_2$to final film thickness h_f of h_2 is

$$\bar{t}=\frac{3w\,h_0^2}{2\mu bL^3}=\int_{h_f}^{1}\left\{K^3\left[G_1\left(N,\overline{h_s},\overline{h_2},L,M_0\right)+\psi\left(\frac{1-N^2}{1+N^2}\right)\right]^{-1}+\left(1-K^3\right)\left[G_2\left(N,\overline{h_2},L,M_0\right)+\psi\left(\frac{1-N^2}{1+N^2}\right)\right]^{-1}\right\}d\bar{h}_2 \tag{22}$$

where $G_1\left(N,\overline{h_s},\overline{h_2},L,M_0\right)=\frac{\overline{a_1}-\overline{b_1}}{M_0^2\overline{A_1}\overline{A_2}\left(\overline{c_1}-\overline{d_1}\right)}$

$$\overline{a_1}=\overline{g_1}\overline{A_1}\,\mathrm{Sinh}\left(\frac{\overline{A_1}\left(\overline{h_s}+\overline{h_2}\right)}{2}\right)\left(\overline{A_2}\left(\overline{h_s}+\overline{h_2}\right)\mathrm{Cosh}\left(\frac{\overline{A_2}\left(\overline{h_s}+\overline{h_2}\right)}{2}\right)-2\,\mathrm{Sinh}\left(\frac{\overline{A_2}\left(\overline{h_s}+\overline{h_2}\right)}{2}\right)\right)$$

$$\overline{b_1}=\overline{g_2}\overline{A_2}\,\mathrm{Sinh}\left(\frac{\overline{A_2}\left(\overline{h_s}+\overline{h_2}\right)}{2}\right)\left(\overline{A_1}\left(\overline{h_s}+\overline{h_2}\right)\mathrm{Cosh}\left(\frac{\overline{A_1}\left(\overline{h_s}+\overline{h_2}\right)}{2}\right)-2\,\mathrm{Sinh}\left(\frac{\overline{A_1}\left(\overline{h_s}+\overline{h_2}\right)}{2}\right)\right)$$

$$\overline{c_1}=\overline{g_1}\,\mathrm{Cosh}\left(\frac{\overline{A_2}\left(\overline{h_s}+\overline{h_2}\right)}{2}\right)\mathrm{Sinh}\left(\frac{\overline{A_1}\left(\overline{h_s}+\overline{h_2}\right)}{2}\right),\overline{d_1}=\overline{g_2}\,\mathrm{Cosh}\left(\frac{\overline{A_1}\left(\overline{h_s}+\overline{h_2}\right)}{2}\right)\mathrm{Sinh}\left(\frac{\overline{A_2}\left(\overline{h_s}+\overline{h_2}\right)}{2}\right)$$

and $G_2\left(N,\overline{h_2},L,M_0\right)=\frac{\overline{a_2}-\overline{b_2}}{M_0^2\overline{A_1}\overline{A_2}\left(\overline{c_2}-\overline{d_2}\right)}$

$$\overline{a_2}=\overline{g_1}\overline{A_1}\,\mathrm{Sinh}\left(\frac{\overline{A_1h_2}}{2}\right)\left(\overline{A_2h_2}\,\mathrm{Cosh}\left(\frac{\overline{A_2h_2}}{2}\right)-2\,\mathrm{Sinh}\left(\frac{\overline{A_2h_2}}{2}\right)\right)$$

$$\overline{b_2}=\overline{g_2}\overline{A_2}\,\mathrm{Sinh}\left(\frac{\overline{A_2h_2}}{2}\right)\left(\overline{A_1h_2}\,\mathrm{Cosh}\left(\frac{\overline{A_1h_2}}{2}\right)-2\,\mathrm{Sinh}\left(\frac{\overline{A_1h_2}}{2}\right)\right)$$

$$\overline{c_2}=\overline{g_1}\,\mathrm{Cosh}\left(\frac{\overline{A_2h_2}}{2}\right)\mathrm{Sinh}\left(\frac{\overline{A_1h_2}}{2}\right),\overline{d_2}=\overline{g_2}\,\mathrm{Cosh}\left(\frac{\overline{A_1h_2}}{2}\right)\mathrm{Sinh}\left(\frac{\overline{A_2h_2}}{2}\right)$$

$$\overline{h_f}=\frac{h_f}{h_0},\overline{h_2}=\frac{h_2}{h_0},\overline{h_s}=\frac{h_s}{h_0}$$

3 Result and discussion

In this study, the lubrication of squeezing film between stepped porous parallel plates lubricated with micropolar fluid in the existence of applied magnetic field M_0 is predicted. MHD and micropolar fluid effect on the squeeze film performance is determined by the parameters the characteristics length L, coupling number N, Hartmann parameter M_0 and permeability parameter ψ. The coupling number N denotes the coupling between the rotational and Newtonian viscosity. Angular and linear momentum equations get decoupled when N is identically zero and the linear momentum equation brings down to the classical Navier-Stokes equations. The influence of an externally applied magnetic field is represented by the magnetization Hartmann number M_0. The permeability parameter is used to investigate the squeeze film performance of stepped porous parallel plates. It is noticed that the problem is limited to the solid case as $\psi\to 0$ and limited to the corresponding Newtonian case as $N,L\to 0$

In the limiting condition, as $M_0\to 0$ the problem brings down to the non-magnetic case of lubricant studied by Siddangouda.[4]

3.1 Magnetohydrodynamic Micropolar fluid Load- Carrying Capacity

The dimensionless load-carrying capacity variation with the non-dimensional film thickness $\bar{h}$for various values of, N,L,M_0 and at two distinct values of permeability parameter $\psi$is presented in Figure 2. When compared to the non-magnetic condition, a magnetic field increases the load on the squeezing film. Furthermore, the impact of the micropolar fluid increases W as compared to the Newtonian condition. For a porous case $(\psi = 0.01)$, compared to a solid case, the permeability parameter diminishes the load capacity. Increasing values of N, L, M_0, and increases the load capacity of the stepped plates.

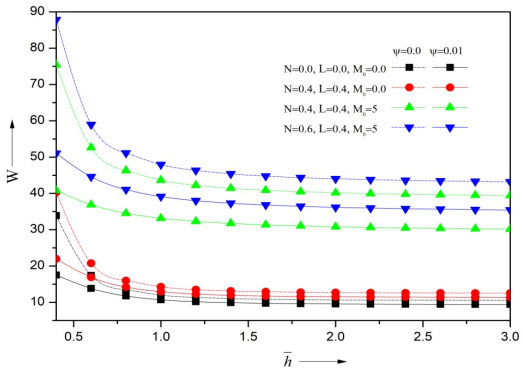

Fig 2. Variation of non-dimensional load W with $\bar{h}$ for different values of N, L, $M_0$with K = 0.5

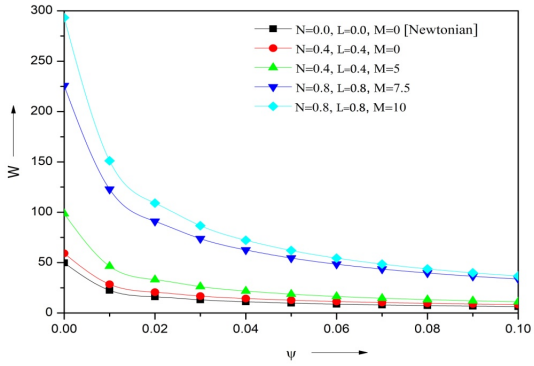

Fig 3. Variation of non-dimensional load W with $\psi$for different values of and N, L, M_0 with $H = 0.4$, $K = 0.5$

Figure 3 illustrates the variation of W with respect to the permeability parameter for distinct values of N, L, M_0. It is noticed in the graph that there is increase in the value of W for increasing values of N, L, M_0, compared to the Newtonian case. For both micropolar and magnetic cases, the load carrying capacity gradually decreases with increasing values of ψ. Figure 4 describes the variation of W with dimensionless film thickness for varied values of K. The load is maximum in solid case $(\psi = 0)$as compared to that of porous case $(\psi = 0.01)$.

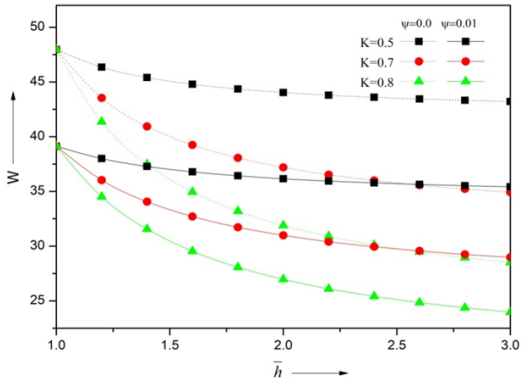

Fig 4. Variation of non-dimensional load W with $\bar{h}$ for different values of K with L = 0.15, N = 0.5, M_0 = 5

3.2 Magnetohydrodynamic micropolar fluid Squeezing Film Time

The time of approach, to reduce the initial film thickness of h_2 of h_0 a final value h_f, is an important feature of the squeeze film bearing. The non-dimensional squeeze film time $\bar{t}$ variation with final film thickness$\overline{h_f}$is shown in Figure 5. Increasing values of N, L, M_0, increases the load capacity W as compared to the Newtonian case. In porous case $(\psi = 0.01)$effect of permeability parameter diminishes the approaching time in comparison with the corresponding solid case $(\psi = 0)$.

Figure 6 denotes the variation of $\bar{t}$with ψ for varied values of N, L, M_0 . We find that there is decrease in the squeeze film time with increasing values of ψ as stepped parallel plates approach each other. The varying values of $\bar{t}$as a function of $\overline{h_f}$for distinct values of K is plotted in Figure 7. A decrease in fluid film thickness with decreasing value of K is found to lead to an increase in the value of squeeze film time. When compared with a non-porous case, the response time decreases for stepped porous parallel plates. The variation of $\bar{t}$with $\overline{h_f}$for varied values of $\overline{h_s}$step height ratio is shown in Figure 8. Increase in the squeeze film time $\bar{t}$can be observed by decreasing step height ratios $\overline{h_s}$. Solid cases have an increased value of $\bar{t}$ as compared to porous cases.

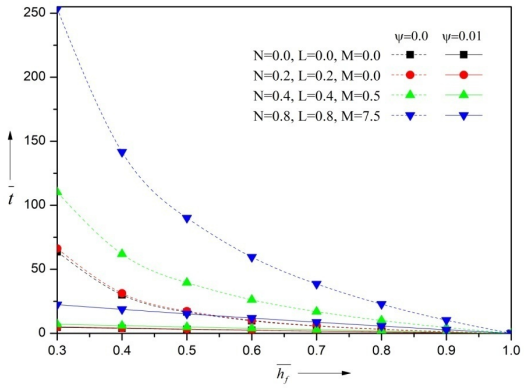

Fig 5. Variation of non-dimensional time of approach $\bar{t}$ with $\overline{h_f}$ for different values of N, L and $M_0$with K = 0.6.

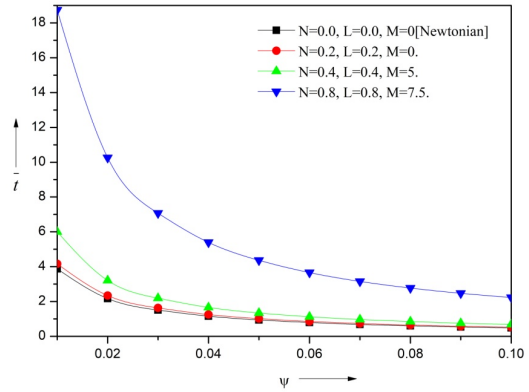

Fig 6. Variation of non-dimensional time of approach with $\psi$for different values of N, L and M_0 with K = 0.6,

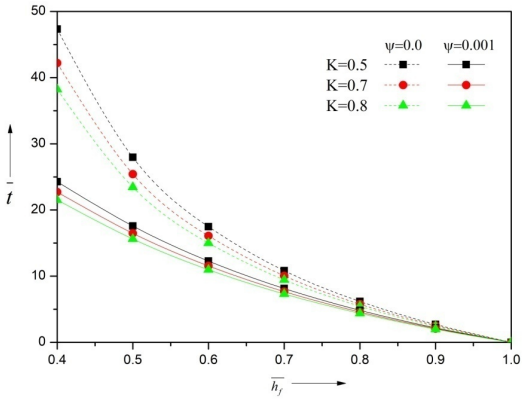

Fig 7. Variation of non-dimensional time of approach $\bar{t}$ with $\overline{h_f}$for different values of K with N = 0.4, L = 0.4, M_0 = 3, and $\overline{h_s}$ = 0.15.

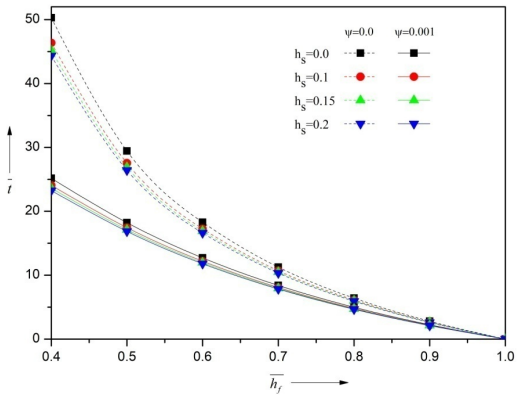

Fig 8. Variation of non-dimensional time of approach $\bar{t}$ with $\overline{h_f}$ for different values of $\overline{h_s}$ with N = 0.4, L = 0.4, M_0 = 3, and K = 0.6.

Table 1 represents the relative percentage increase due to magnetic effect in load carrying capacity R_{w^*}, for two distinct values of ψ and Hartmann number M and is given by the relation $R_{W^*} = \frac{W^*_{\text{magnefic}} - W^*_{\text{non-magnetic}}}{W^*_{\text{non-magnetic}}} \times 100$. It is observed that, for $M = 5$, $h = 1$ the load capacity increases by 156.5% and 49.5% as compared to the non-magnetic case for $\psi = 0.01$ and 0.1 respectively. It is concluded that increasing value of the permeability parameter diminishes the load capacity.

Table 1. The variation of relative Load R_{w^*} for the various values of ψ and M_0

ψ	h	$M_0 = 3$	$M_0 = 5$	$M_0 = 7.5$	$M_0 = 10$
0.01	0.6	48.07	118.25	218.01	310.54
	1.0	63.472	156.47	289.40	413.52
	1.4	67.173	165.89	307.87	441.61
0.1	0.6	22.38	41.67	57.13	65.77
	1.0	26.69	49.498	67.59	77.624
	1.4	30.22	55.87	76.18	87.42

Table 2 represents the relative percentage increase due to magnetic effect in dimensionless squeeze film time R_{t^*} for distinct values of ψ and Hartmann number M and is given by the relation. $R_{t^*} = \frac{t^*_{\text{magnetic}} - t^*_{\text{non-magnetic}}}{t^*_{\text{non-magnetic}}} \times 100$. It is observed that, for $M = 5$, $h = 1$ the squeeze film time increases by 23.3% and 2.9% in comparison with the non-magnetic case for $\psi = 0.01$ and 0.1 respectively.

Table 2. The variation of relative time R_{t^*} for the various values of ψ and M_0.

ψ	h_f	$M_0 = 3$	$M_0 = 5$	$M_0 = 7.5$	$M_0 = 10$
0.01	0.4	8.379	15.90	22.23	25.901
	0.6	12.45	23.30	32.11	37.074
	0.8	18.47	33.918	46	52.627
0.1	0.4	1.25	2.13	2.76	3.094
	0.6	1.769	2.973	3.798	4.216
	0.8	2.59	4.239	5.296	5.811

4 Conclusion

Using micropolar fluids and applied magnetic fields, this study examines the squeeze film lubrication of stepped porous parallel plates. In the limiting case as $N, L \to 0$, the results of Newtonian case can be recovered. From the results discussed in the previous

section the following conclusions are drawn:

1. The enhanced load carrying capacity and delayed time of approach are observed for the micropolar fluids in comparison with the Newtonian case.
2. The effect of applied magnetic field increases W and $\bar{t}$.
3. The presence of porous facing on the bearing surface decreases W and $\bar{t}$. However, the proper choice of lubricant additive and strength of applied magnetic field, this loss can be compensated and the performance of the squeeze film can be improved.

5 Nomenclature

$\overline{h}$ dimensionless mean film thickness (=h/h_2)
h_1 maximum film thickness
h_2 minimum film thickness
$\overline{h_s}$ step height (=h_s/h_0)
KL step position, $0<K<1$.
L dimensionless characteristic length $\left(=(\gamma/4\mu)^{1/2}/h_2\right)$
N coupling number $\left(=(\chi/\chi+2\mu)^{1/2}\right)$
M_o Hartmann number
p film region pressure
$\overline{p}$ expected value of p
P dimensionless pressure, $P=\frac{\bar{p}h_2^3}{\mu VL^2}$
$\overline{p}_1$ pressure in the region $0\le x\le KL$.
$\overline{p}_2$ pressure in the region $KL\le x\le L$.
t squeeze film time
$\bar{t}$ Non-dimensional squeeze film time $\left(=\frac{2w\ h_0^2t}{3\mu bL^3}\right)$
V squeezing velocity
w load carrying capacity
W non-dimensional load carrying capacity $\left(=\frac{2W\ h_2^3}{3\mu bVL^3}\right)$
χspin viscosity
δ thickness of porous layer
γ viscosity coefficient of micropolar fluids
μ Newtonian viscosity coefficient
ϕ^* permeability
ψ permeability parameter $\left(=\phi^*\delta/h_2^3\right)$

References

1) Hays DF. Squeeze Films for Rectangular Plates. *Journal of Basic Engineering*. 1963;85(2):243–246. Available from: https://doi.org/10.1115/1.3656568.
2) Wu H. An Analysis of the Squeeze Film Between Porous Rectangular Plates. *Journal of Lubrication Technology*. 1972;94(1):64–68. Available from: https://doi.org/10.1115/1.3451637.
3) Singh P, Radhakrishnan V, Narayan KA. Squeezing flow between parallel plates. *Ingenieur-Archiv*. 1990;60(4):274–281. Available from: https://doi.org/10.1007/BF00577864.
4) Siddangouda A. Squeezing Film Characteristics for Micropolar Fluid between Porous Parallel Stepped Plates. *Tribology in Indrustry*. 2015;37(1):97–106. Available from: http://www.tribology.rs/journals/2015/2015-1/13.pdf.
5) Naduvinamani NB, Apparao S, Gundayya HA, Biradar SN. Effect of Pressure Dependent Viscosity on Couple Stress Squeeze Film Lubrication between Rough Parallel Plates. *Tribology Online*. 2015;10(1):76–83. Available from: https://doi.org/10.2474/trol.10.76.
6) Patel JR, Deheri G. Combined Effect of Slip Velocity and Roughness on the Jenkins Model Based Ferrofluid Lubrication of a Curved Rough Annular Squeeze Film. *Journal of Applied Fluid Mechanics*. 2016;9(2):855–865. Available from: https://doi.org/10.18869/acadpub.jafm.68.225.24447.
7) Hanumagowda BN, Shivakumar HM, Raju BT, Kumar JS. Combined Effect of Pressure-Dependent Viscosity and Micropolar Fluids on Squeeze Film Circular Stepped Plates. *International Journal of Mathematics Trends and Technology*. 2016;37:175–183. Available from: https://doi.org/10.14445/22315373/IJMTT-V37P523.
8) Madalli VS, Patil S, Hiremath A, Kudenatti R. Analysis of the viscosity dependent parameters of couple stress fluid in porous parallel plates. *Industrial Lubrication and Tribology*. 2018;70(6):1086–1093. Available from: https://doi.org/10.1108/ILT-10-2017-0315.

9) Hanumagowda BN, Karappan SC. Stochastic Reynolds equation for the combined effects of piezo-viscous dependency and squeeze film lubrication of micropolar fluids on rough porous circular stepped plates, Proceedings of the Institution of Mechanical Engineers. *Part J: Journal of Engineering Tribology*. 2022;2022(4):748–758. Available from: https://doi.org/10.1177/13506501211022452.
10) Anagod RR, Kumar JS, Hanumagowda BN. Squeeze film behavior of rough elliptical plates with micropolar fluids. *ARPN Journal of Engineering and Applied Sciences*. 2018;13(23). Available from: http://www.arpnjournals.org/jeas/research_papers/rp_2018/jeas_1218_7434.pdf.
11) Jahan N, Hanumagowda BN, Salma A, Shivakumar HM. Combined effect of piezo-viscous dependency and Couple Stresses on Squeeze-Film Characteristics of Rough Annular Plates. *Journal of Physics: Conference Series*. 2018;1000:012082. Available from: https://doi.org/10.1088/1742-6596/1000/1/012082.
12) Goud BS, Reddy YD, Alshehri NA, Jamshed W, Safdar R, Eid MR, et al. Numerical Case Study of Chemical Reaction Impact on MHD Micropolar Fluid Flow Past over a Vertical Riga Plate. *Materials*. 2022;15(12):4060. Available from: https://doi.org/10.3390/ma15124060.
13) Eringen AC. Theory of Micropolar Fluids. *Indiana University Mathematics Journal*. 1966;16(1):1–18. Available from: https://www.jstor.org/stable/24901466.
14) Hughes WF. Magnetohydrodynamic lubrication and its application to liquid metals. *Industrial Lubrication and Tribology*. 1963;15(3):125–133. Available from: https://doi.org/10.1108/eb052722.
15) Kuzma DC, Maki ER, Donnelly RJ. The magnetohydrodynamic squeeze film. *Journal of Fluid Mechanics*. 1964;19(3):395–400. Available from: https://doi.org/10.1017/S0022112064000805.
16) Hamza EA. The Magnetohydrodynamic Squeeze Film. *Journal of Tribology*. 1988;110(2):375–377. Available from: https://doi.org/10.1115/1.3261636.
17) Lin JR, Chu LM, Hung CR, Lu RF. Magneto-Hydrodynamic Non-Newtonian Curved Circular Squeeze Films. *Journal of Marine Science and Technology*. 2014;22(5):566–571. Available from: https://doi.org/10.6119/JMST-013-0716-2.
18) Islam S, Khan A, Deebani W, Bonyah E, Alreshidi NA, Shah Z. Influences of Hall current and radiation on MHD micropolar non-Newtonian hybrid nanofluid flow between two surfaces. *AIP Advances*. 2020;10(5):055015. Available from: https://doi.org/10.1063/1.5145298.
19) Halambi B, Hanumagowda B. Effect of Hydromagnetic Squeeze Film Lubrication Of Micropolar Fluid Between Two Elliptical Plates. *International Journal of Mechanical Engineering and Technology (IJMET)*. 2018;9(8):939–947. Available from: http://iaeme.com/Home/issue/IJMET?Volume=9&Issue=8.
20) Zahir S, Meshal S, Abdullah D, Poom K, Thounthong P, Saeed I. Impact of Cattaneo-Christov heat flux on non-isothermal convective micropolar fluid flow in a hall MHD generator system. *J Materi Res Technol*. 2020;9(3):5452–5462. Available from: https://doi.org/10.1016/j.jmrt.2020.03.071.
21) Zahir S, Mccash LB, Abdullah D, Ebenezer B. Entropy optimization in Darcy-Forchheimer MHD flow of water based copper and silver nanofluids with Joule heating and viscous dissipation effects. *AIP Advances*. 2020;10(065137). Available from: https://doi.org/10.1063/5.0014952.
22) Biradar T, Hanumagowda BN, Suresh B. Biradar Kashinath, Patil Vishal, Effect of MHD and couple stress on squeeze film characteristics between porous curved annular circular plates. *International Journal of Mechanical and Production Engineering Research and Development*. 2020;10(3):8535–8546. Available from: http://www.tjprc.org/publishpapers/2-67-1601018265-811IJMPERDJUN2020811.pdf.
23) Qui-Hong S, Tayyaba S, Mushtaq M, Ijaz MK, Zahir S. Kumam Poom, Modelling and numerical computation for flow of micropolar fluid towards an exponential curved surface: a keller box method. *Scientific reports*. 2021;11(16351). Available from: https://doi.org/10.1038/s41598-021-95859-x.
24) Vandana Agarwal, Singh B, Kumari A, Jamshed W, Nisar KS, Almaliki AH, et al. Steady Magnetohydrodynamic Micropolar Fluid Flow and Heat and Mass Transfer in Permeable Channel with Thermal Radiation. *Coatings*. 2022;12(1):11. Available from: https://doi.org/10.3390/coatings12010011.
25) Ullah H, Shoaib M, Akbar A, Raja MAZ, Islam S, Nisar KS. Neuro-Computing for Hall Current and MHD Effects on the Flow of Micro-Polar Nano-Fluid Between Two Parallel Rotating Plates. *Arabian Journal for Science and Engineering*. 2022;24:1–21. Available from: https://doi.org/10.1007/s13369-022-06925-z.